

On the Commonality between Theoretical Models for Fluid and Solid Friction, Wear and Tribochemistry

Hugh Spikes¹ and Wilfred Tysoe²

¹*Tribology Section, Department of Mechanical Engineering, Imperial College, London SW7 2AZ, UK*

²*Department of Chemistry and Biochemistry, University of Wisconsin-Milwaukee, Milwaukee, WI 53211, USA*

ABSTRACT

Tribology is concerned with the influence of mechanically-applied forces on interfacial phenomena that accompany and control sliding. A wide range of models have been developed to describe these phenomena, which include frictional dissipation, wear and tribochemical reactions. This paper shows that these apparently disparate models are based on the same fundamental concept; that an externally applied force accelerates the rate of thermal transition of atoms or molecules across energy barriers present in solid and liquid materials, thereby promoting flow, slip or bond cleavage. Such “stress-assisted” effects and the associated thermal activation concepts were developed independently and in different forms by Prandtl in 1928 [1] and Eyring in 1936 [2]. These two works have underpinned subsequent theories of dry friction, boundary lubrication, EHD rheology, tribochemistry and nanoscale wear modelling.

This paper first reviews the historical development of the concepts, focussing in particular on the models of Prandtl and Eyring and how they have subsequently been used and adapted by others. The two approaches are then compared and contrasted, noting that although superficially similar, they contain quite different assumptions and constraints. First, the Prandtl model assumes that the force is exerted through a compliant spring, while constant-force sliding is assumed by Eyring. Second, different approximations are made in the two models to describe the change in energy barrier with external force. Prandtl explores the asymptotic behaviour of the energy barrier as the applied force become sufficiently high to reduce it to zero, while Eyring assumes that the energy barrier is reduced by an amount equal to the external work carried out on the system. The theoretical underpinnings of these differences are discussed along with the implications of compliant coupling and constant-force sliding on the velocity and temperature dependence of the friction forces for the two models.

KEYWORDS: Prandtl friction model, Eyring viscosity model, wear, fracture, tribochemistry.

1. INTRODUCTION

Tribology is concerned with the influence of mechanically applied forces on interfacial phenomena that accompany and control sliding, including frictional dissipation, wear and tribochemical reactions. A wide range of models have been developed to describe these phenomena. Fundamentally, however, they all aim to understand the way in which an external force affects the state of a solid or liquid at a sliding interface, so that the underlying principles of these models are essentially identical, although often framed in somewhat different language. The aim of this paper is to highlight the commonality between many apparently disparate tribological models that are used to describe dry friction, boundary friction, elasto-hydrodynamic friction, wear and tribochemical reactions.

The equilibrium state of a material and the associated thermodynamic potentials (enthalpy, entropy, Gibbs free energy, *etc.*) can be calculated from first principles using statistical thermodynamics [3]. Much of physics and chemistry is concerned with the way in which the equilibrium state is modified by the application of some external potential, for example an electric field, pressure or change in chemical potential. In the case of relatively small perturbations, the change is completely reversible; removal of the external potential restores the initial, unperturbed state and can be modelled by non-equilibrium thermodynamics [4] or perturbation theory [5]. In the case of external forces acting on solid materials, the mechanical response is expressed by the elastic moduli.

In many cases of interest, particularly for sliding interfaces, the mechanical forces are often sufficiently large that the initial, equilibrium state is driven over some metastable state into another configuration. This was first realized by Prandtl in 1928 in the context of crystal plasticity, although he pointed out that similar concepts would apply equally well to sliding interfaces [1]. In 1929 Tomlinson developed a very similar concept based on inter-atomic forces and which was directed specifically at explaining sliding friction [6]. The combined approach is now widely known as the Prandtl-Tomlinson model. The energy of this metastable state is known in chemical reaction rate theory as the activation energy ΔH^\ddagger . The rate at which a system can surmount this energy barrier at some temperature T depends on the proportion of the system that has an energy higher than ΔH^\ddagger . At equilibrium, this is given by a Boltzmann energy distribution, which yields a transition rate over the barrier that is proportional to $Ae^{-\frac{\Delta H^\ddagger}{k_B T}}$, where k_B is the Boltzmann constant, and A is a pre-exponential factor with units of seconds⁻¹ and can be thought of as an attempt frequency. The central concept in describing the effect of an external force on the rate of the process is to realize that the external force F can carry out work $W(F)$ on the system to reduce the activation barrier from ΔH^\ddagger to $\Delta H^\ddagger - W(F)$, thereby increasing the rate at which the system transits the barrier in the direction of the applied force by a factor $e^{\frac{W(F)}{k_B T}}$. The same principle was also exploited by Eyring in the development of a model of liquid viscosity in 1936 [2]. It should be emphasized that the process is still thermally activated but that the external

force reduces the energy barrier that must be surmounted. Consequently, they will be referred to in the following as stress-assisted effects.

The goal of this paper is to point out that this concept, in various guises, has been used to describe a wide range of tribological phenomena and to compare the approaches used. While similar effects will occur in general under the influence of an external force, such as when pulling to cause bond scission, or fracture, we restrict our discussion primarily to those phenomena that occur under the influence of a shear force that is parallel to the contacting interface imposed during sliding.

The discussion of shear-assisted effects is divided into two general classes; (1) those processes in which the final state, after having transited the energy (activation) barrier, is degenerate with the initial state, and (2) those for which it is not. When the initial and final states are degenerate, no structural evolution of the system will have occurred after transit of the energy barrier, only energy dissipation. In this case, the applied force is just the friction force. However, if the final state energy differs from the initial state, this must be accompanied by a structural evolution, such as occurs during wear or a chemical reaction.

The paper is in two parts. In the first we adopt an historical approach to describe how the ideas proposed by Prandtl and Eyring described above have been developed and applied, first to degenerate and later to non-degenerate tribological processes. Here we preserve the original notation used for each approach and point out when different symbols are used to describe similar parameters. They are also tabulated (see Table 1) for convenience.

In the second, Discussion part of the paper, the approaches of Prandtl and Eyring are compared and contrasted, in particular their respective treatments of the effect of applied force on the energy barrier. The first significant difference is that Prandtl assumes that the force is coupled elastically, while Eyring assumes a constant force. Prandtl's approach is especially applicable to the analysis of AFM friction (the Prandtl-Tomlinson model) since the AFM tip can be considered as a moving contact constrained by an elastic cantilever, while constant-force sliding is relevant to macroscopic interfaces. The second difference lies in the fact that the problem of calculating the change in energy barrier as a function of the external force cannot be solved exactly, even for a simple sinusoidal energy profile. This requires the use of approximate solutions that are different in the Prandtl and Eyring models. Treatments are presented to compare both elastic and constant-force sliding and the approximations used to calculate force-dependent energy barriers and their application to both the Prandtl-Tomlinson friction and Eyring's viscosity models and the models that derive from them.

2. DEGENERATE INITIAL AND FINAL STATES; FRICTION FORCES

2.1 Prandtl/Tomlinson Model for Sliding Friction

In 1928, Prandtl developed a model of crystal plasticity [1] based on the forces experienced, and consequent motion of a point mass constrained in an elastic surface as this surface slides across the periodic force field created by the particles in a parallel counter-surface. Although intended primarily to model plastic deformation, in last few paragraphs of his paper Prandtl also briefly noted its applicability to sliding friction. This remarkable paper will be outlined in some detail since, together with Eyring's work to be described in the next section, it underpins, or at least anticipates most modern attempts to model sliding friction.

Prandtl's paper is effectively divided into two parts. In the first, he shows that for incommensurate surfaces the combination of attractive and repulsive forces acting on individual point masses (atoms) can lead to instability in their sliding motion as they pass over potential barriers, so that they jump from one stable state to another, producing a consequently irreversible, energy-dissipating process. Prandtl illustrates this behaviour using the experimental model shown in Fig. 1.

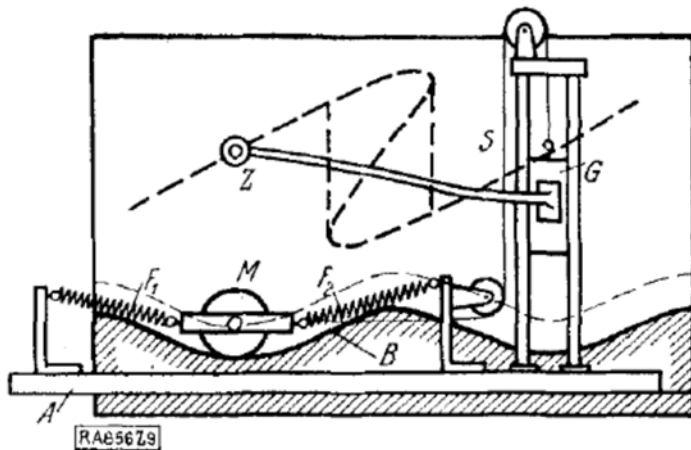


Figure 1: Depiction of the Prandtl machine, reproduced with permission from [1].

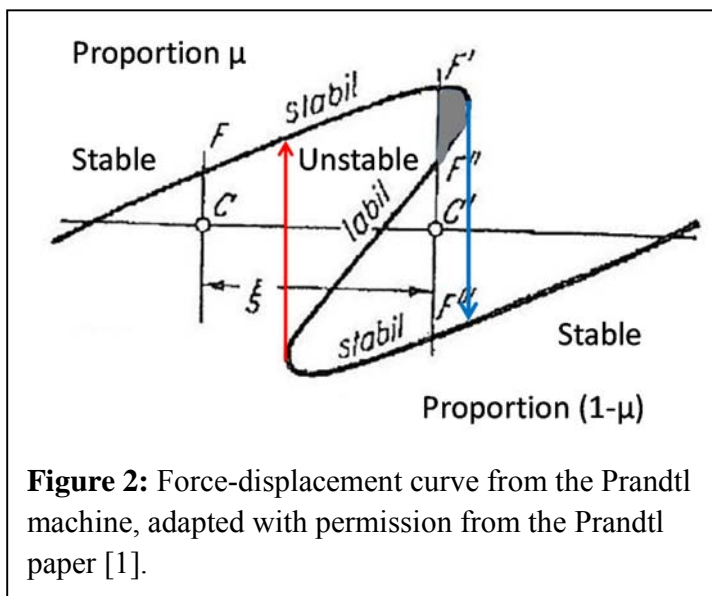
Here, a flat substrate (A) moves horizontally, and is attached through two springs (F_1 and F_2) to a heavy roller (M) which represents an elastically-constrained point mass. The substrate can be moved horizontally (a distance ζ in the $\pm x$ directions) against another straight edge (B) that has an undulating surface to represent the periodic potential. To represent the motion that occurs when the slider A moves, the roller M is attached by a cord S via two pulleys, to a weight G . The pulleys are rigidly attached to the slider A . An arm with a pointer Z is attached to the weight G to plot out curves used to analyze the model, presumably, in 1928 by attaching a piece of chalk to the pointer. The horizontal motion of the pointer corresponds to the rigid displacement of the sliding substrate A .

Now, as the slider moves, it pulls the mass M some distance X , such that the weight G moves vertically a distance $(X-\zeta)$. If the combined force constant of the springs is k , then the restoring force is $-k(X-\zeta)$ so that the vertical displacement in the Prandtl machine corresponds to

the force acting on the system. Initially, motion of the slider A produces a restoring force that increases as the slider is displaced, resulting in a stable region where the force on the springs are balance by the restoring force of the mass M on the slope.

However when the force field is relatively strong and the elastic constraint weak, there is a point of instability when the mass jumps from one position to another as illustrated by the blue line in Prandtl's force-displacement curve shown in Fig. 2.

Reversing the motion will cause the curve to trace along the lower stable position until it reaches the inflection point once again, to move back to the original stable position along the red line. Accordingly, there is a metastable (*labil*) region between the two points. In the regions between these two points, during displacement ξ from C to C' , for example, there are three equilibrium states, F' , F'' and F''' , two of which are stable. The energy of the system at some point is $\int F(\xi)d\xi$ and is therefore given by the area under the curve.



Prandtl applied this model to explore hysteresis effects in inelastic stress-strain behaviour but it can also be considered as explaining the origins of dissipative sliding friction. However the above explanation of sliding friction represents only the first of Prandtl's innovations. In the second part of his 1928 paper he then considers what he refers to as "time effects" by coupling the influences of both thermal and mechanical effects to predict the movement of atoms over the energy barrier and thus the rate of deformation or sliding. Prandtl recognised that, as atoms are forced up the "stabil" part of the force-distance curve shown in Fig. 2, there is an increasing probability that they will possess enough thermal energy to surmount the remainder of the barrier without further application of force. In Fig. 2, if the slider is displaced to position F' , it will require further energy U , the area under the curve to the right of $F'F''$ and shown as the shaded, grey area, to transition to F'' . The probability W of thermally undergoing this transition is $W \propto$

$e^{-\frac{U}{k_B T}}$ (Prandtl actually used the term U_m , the “the average value of the oscillatory energy of the particle” in place of $k_B T$).

Prandtl then considers a large ensemble of particles at one position ξ , with fraction μ in the upper position (see Fig. 2) and $(1-\mu)$, in the lower position, and assumes a transition time, τ , which he suggests is of the same order of magnitude as the period of oscillation of the particles. Thus, the rate of increase in the fraction of particles in the upper position is simply the rate of transfer from lower to upper positions minus the rate of transfer from upper to lower, where the positions are shown in Fig. 2, i.e.

$$\frac{d\mu}{dt} = \frac{1}{\tau} \left((1 - \mu) e^{-\frac{U_2}{k_B T}} - \mu e^{-\frac{U_1}{k_B T}} \right) \quad (3)$$

U_1 is the energy needed to reach the unstable position from the upper position, and U_2 is that needed from the lower position, so the equation considers forward and reverse motions. For a steady rate of deformation (or sliding speed in the case of friction) $d\mu/dt$ can be replaced by $d\mu/dx \cdot dx/dt$ so Equ. 3 becomes;

$$\frac{d\mu}{dx} = \frac{1}{\tau c} \left((1 - \mu) e^{-\frac{U_2}{k_B T}} - \mu e^{-\frac{U_1}{k_B T}} \right) \quad (4)$$

where c is the deformation rate or sliding speed, dx/dt .

Solution of Equ. 4 requires expressions for the variation of the values of U_1 and U_2 with displacement. Prandtl notes that for a sinusoidal sliding potential, the balance between the elastic force (proportional to x) and the gradient of the potential (a sinusoid), leads to a transcendental equation. He thus makes two alternative simplifying approximations. In the first, he expands the shaded area in Fig. 2 as a Taylor series as a function of x to give $\frac{U_1}{k_B T} = A - Bx$ and $\frac{U_2}{k_B T} = A + Bx$. Even with this extreme simplification, Equ. 4 could only be solved if the

first term was considered negligible, giving; $\frac{1}{\mu} \frac{d\mu}{dx} = -\frac{e^{-A}}{c\tau} e^{Bx}$. Prandtl integrates this expression

twice, first to determine $\mu(x) = e^{-\frac{1}{Bc\tau e^{-A}} e^{Bx}}$, and then over the “stabil” region from $x=0$ to a , where a is the value of x at the critical position where spontaneous sliding occurs, to determine the total force required to provide a constant deformation rate c . He obtains a relationship between the applied force, P and the deformation rate or sliding speed, c of the form;

$$P = \frac{P_{\max}}{aB} (\ln(c) + A + \ln(B\tau) - 0.5772) \quad (5)$$

where P_{max} is the applied force at which spontaneous sliding occurs. The constant -0.5772 originates from the integration process and is the value of $\int_0^1 \ln(-\ln \mu) d\mu$. As will be seen in this review, and indeed as Prandtl notes, this linear-logarithmic form is characteristic of the relationship between force and speed for many sliding contacts.

Prandtl also proposes a more accurate asymptotic approximation for $U(x)$ by approximating the shaded area in Fig. 2 as a parabola. Then the forces F at positions F' and F'' in Fig. 2 can be written as: $(a-x) = \frac{F(x)^2}{\alpha^2}$, where α is a constant. Putting $a - x = y$ and integrating gives;

$$U = \int F(x) dx = \alpha \int y^{1/2} dy = \frac{2}{3} \alpha (x - a)^{3/2} \quad (6)$$

Assuming that $U = kT$ at a point from the transition given by $a - x = b$ gives a more convenient formula for U as: $\frac{U}{k_B T} = \left(\frac{a-x}{b}\right)^{3/2}$.

This can be substituted into the above rate equation and integrated directly as:

$$\ln \mu(x) = -\frac{1}{c\tau} \int_{-\infty}^x e^{-\left(\frac{a-x'}{b}\right)^{3/2}} dx' \quad (7)$$

This integral cannot be solved exactly, but Prandtl provides a series solution.

Prandtl also discusses the impact of temperature on deformation rate according to his model and notes that his assumption of a parabolic form of $U(x)$ predicts that the applied force to give constant deformation, or sliding rate, will decrease with temperature according to;

$$P = a_1 - a_2 T^{2/3} \quad (8)$$

Prandtl's model outlined above received relatively little attention until the 1990s. Unfortunately, its approach, which involves integration of the probability of transition twice, both locally and over the approach distance, precludes many analytical solutions. Prandtl could show that applied force varies linearly with deformation rate at high temperatures and low rates, and that it varies logarithmically at high applied forces, when the reverse term in Equ. 4 can be neglected. But in the absence of numerical computers in 1928, further solution was not practicable.

However, with the growth of interest in nanotribology in the 1990s, the significance of Prandtl's "time effects" in describing the impact of both sliding speed and temperature on dry friction was recognised. Since then Prandtl's approach has been very widely employed to analyse friction in atomic force microscopes (AFMs) [7-11], while Müser has argued its application to model the sliding between two confined liquid layers at high pressure [12].

2.2 Eyring Model for Viscosity and Shear Thinning of Liquids

Early models of liquid viscosity were based on the momentum transfer concepts used to explain gas viscosity, but these were not realistic for dense fluids. In 1936 Eyring developed a molecular model of liquid viscosity based on activated flow [2]. He started from the transition-state theory of absolute reaction rates that he developed in the preceding year to model chemical kinetics [13] and considered liquid flow as a unimolecular, “chemical” reaction in which the elementary process is a molecule passing from one equilibrium position to another, identical state over an energy barrier [2,14]. A molecule moves approximately one molecular distance, λ into a neighbouring hole in the liquid as shown in Fig. 3(a). If no external force is applied, the rate k at which a molecule transits the energy barrier and hence moves in either direction is given by;

$$k = Re^{-E_a/k_B T} \quad (9)$$

where E_a is the thermal activation energy for flow and R is a pre-exponential factor that depends on the ratio of the partition functions of the activated and initial states.

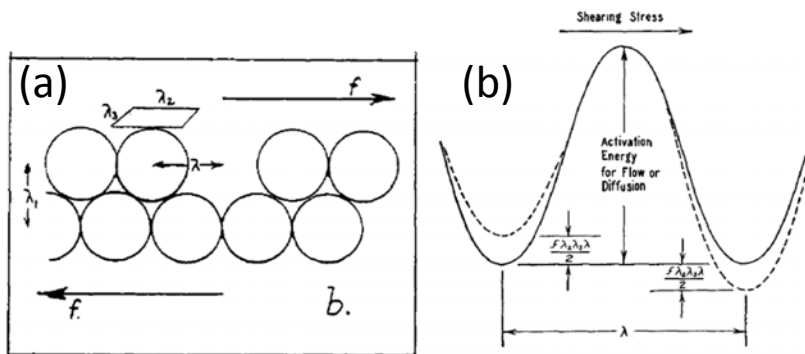


Figure 3: Schematic description of the Eyring model for viscosity [15,14]. Reprinted with permission from [15]. Copyright 1940 American Chemical Society.

When a shear force is applied, this has the effect of lowering the effective activation energy for a flow process in the direction of the force and increasing it in the reverse direction, as shown in Fig. 3(b). Eyring assumed that the energy barrier is raised and lowered by the work done in moving the molecule to the midpoint of the energy barrier (the transition state), *i.e.* $F\lambda/2$, where F is the applied shear force on the molecule and $\lambda/2$ is the distance the molecule moves.

The specific flow rates in the forward and backward directions, k_f and k_b are therefore given by:

$$k_f = Be^{-(E_a - F\lambda/2)/k_B T} = ke^{F\lambda/2k_B T} \quad (10)$$

and

$$k_b = Be^{-(E_a + F\lambda/2)/k_B T} = ke^{-F/2k_B T} \quad (11)$$

Since each time that a molecule pass over a potential barrier it moves a distance λ , the rate of motion of the molecule relative to the neighbouring layer ΔV is given by;

$$\begin{aligned} \Delta u &= k\lambda(k_f - k_b) \\ &= k\lambda(e^{F\lambda/2k_B T} - e^{-F\lambda/2k_B T}) \\ &= 2k\lambda \sinh\left(\frac{F\lambda}{2k_B T}\right) \end{aligned} \quad (12)$$

The shear rate is given by the difference in velocity divided by the spacing between layers, λ_1 , while Eyring equates the shear force, F , on the molecule to the shear stress, f , by $F = f\lambda_2\lambda_3$ where λ_2 and λ_3 are the lengths of the molecule (or flow unit) in the direction of applied force and the transverse direction respectively. This gives;

$$\dot{\gamma} = \frac{\Delta u}{\lambda_1} = \frac{2k\lambda}{\lambda_1} \sinh\left(\frac{f\lambda_2\lambda_3\lambda}{2k_B T}\right) \quad (13)$$

The effective viscosity is the shear stress divided by the strain rate;

$$\eta_e = \frac{f}{\dot{\gamma}} = \frac{f\lambda_1}{2k\lambda \sinh\left(\frac{f\lambda_2\lambda_3\lambda}{2k_B T}\right)} \quad (14)$$

At low shear stresses, when $f \ll k_B T / \lambda_2\lambda_3\lambda$, $\sinh\left(\frac{f\lambda_2\lambda_3\lambda}{2k_B T}\right) = \frac{f\lambda_2\lambda_3\lambda}{2k_B T}$ so the (Newtonian)

viscosity is given by;

$$\eta_N = \frac{k_B T \lambda_1}{k \lambda_2 \lambda_3 \lambda^2} \quad (15)$$

Eyring then expanded the thermal rate constant k to obtain an expression for viscosity in terms of free volume and enthalpy of vaporisation. Eyring found that for liquids comprising approximately spherical molecules Equ. 15 predicted the measured Newtonian viscosity quite closely based on $\lambda_1, \lambda_2, \lambda_3$ being the dimensions of the molecules, but that it predicted too low a viscosity for polymeric molecules [15]. He suggested that this was because in the latter case the flow unit was only a segment of the molecule. Subsequently the model was modified to take account of elongated molecules, molecular aggregates, high polymer melts and, by assuming multiple flow units with different properties, polymer solutions and colloids [14].

Eyring's model of liquid viscosity has, to some extent, been superseded by more complex models, although it has recently been applied to predict the energy of vaporisation and thus the volatility of lubricants from their viscosities [16]. However his model had an important "by-product" in that it provided the first molecular-based model of shear thinning (pseudoplastic) behaviour of liquids, where, at high shear stresses, the ratio of shear stress to strain rate decreases reversibly with increasing shear stress. Substituting Equ. 15 into Equ. 13 and replacing Eyring's shear stress, f , by the more modern terminology, τ , gives;

$$\dot{\gamma} = \frac{2k_B T}{\eta_N \lambda_2 \lambda_3 \lambda} \sinh\left(\frac{\tau \lambda_2 \lambda_3 \lambda}{2k_B T}\right) \quad (16)$$

If we set $2k_B T / \lambda_2 \lambda_3 \lambda = \tau_e$, the "Eyring stress", this becomes the non-linear relationship between stress and strain;

$$\dot{\gamma} = \frac{\tau_e}{\eta} \sinh\left(\frac{\tau}{\tau_e}\right) \quad (17)$$

In the decade or so after it was developed, this equation was applied with varying degrees of success to describe the shear-thinning properties of polymer melts, solutions and colloids, for which, being a model based on simple, quasi-spherical molecules, it was arguably not suited [17]. Eventually it was superseded for this purpose by network-based models of shear thinning.

However since the 1970s, the Eyring sinh-based relationship between strain rate and shear stress has become very widely used to describe the shear stress/strain rate behaviour of liquid lubricant films in high-pressure elastohydrodynamic (EHD) contacts and thus the frictional properties of such contacts [18]. In EHD lubrication, the extremely high local pressures within the lubricated contact result in a very large viscosity increase which, at high strain rates, gives rise to very large shear stresses. Under these conditions, even simple molecular liquids show extensive shear thinning. It is found that EHD friction (or mean shear stress) *versus* strain rate closely follows an "arsinh" relationship over a wide range of shear rates, in accord with Equ.17. At very high shear stresses this results in friction being proportional to log(strain rate).

Although Eyring's model was developed to describe liquid viscosity, essentially it describes the sliding speed/shear stress relationship between layers of molecules. As such it was adapted by Briscoe and Evans in 1982 to interpret boundary friction between opposing Langmuir-Blodgett monolayers in a surface forces apparatus [19]. They assumed that hydrostatic pressure will increase the height of the energy barrier so that the sliding speed becomes;

$$\begin{aligned}\Delta u &= vb \left(e^{-(E_o + p\Omega - \tau\phi)/k_B T} - e^{(E_o + p\Omega - \tau\phi)/k_B T} \right) \\ &= 2vb e^{-(E_o + p\Omega)/k_B T} \sinh \left(\frac{\tau\phi}{k_B T} \right)\end{aligned}\quad (18)$$

where Q' is the thermal activation barrier, ν is the effective vibration frequency of the sliding molecules, b is the distance across the energy barrier, ϕ is the shear activation volume, equivalent to Eyring's $\lambda\lambda_2\lambda_3/2$, and Ω also has units of volume and is termed the pressure activation volume. At large applied shear stresses when $e^{\sigma\phi} \gg e^{-\sigma\phi}$ this equation reduces to;

$$\Delta u = vb e^{-(E_o + p\Omega)/k_B T} e^{\tau\phi/k_B T} \quad (19)$$

or

$$\tau = \frac{k_B T}{\phi} \log \left(\frac{\Delta u}{vb} \right) + \frac{1}{\phi} (E_o + p\Omega) \quad (20)$$

so that the shear stress and thus the friction coefficient depends on the logarithm of the sliding speed. Equ. 20 also predicts that the shear stress increases linearly with pressure and, since $\Delta u < vb$, decreases linearly with temperature. Briscoe and Evans found good agreement between this equation and experimental measurements of friction between monolayers of fatty acid soaps in glass/mica contacts. Recently Eyring's model has been applied in a very similar fashion to analyse friction behaviour of grafted polymer surfaces in an AFM [20].

Most applications of Eyring's model to sliding friction have considered the forward flow process to dominate, leading to a logarithmic dependence of friction on sliding velocity. However a recent study by Müser used molecular dynamics simulation to predict dry friction over a very wide sliding velocity range and obtained an arsinh dependence of shear stress on velocity extending down to low sliding velocities [21]. Although Müser did not interpret this explicitly in the context of the combined forward and reverse transitions, similarity to the prediction of Eyring's model is striking.

2.3 Schallamach Model

In 1951, Shallamach developed a model to describe the friction of rubber sliding on ground glass [22]. Like Eyring, he interpreted sliding as an activated slip process whose rate and thus the sliding velocity could be described under high levels of tangential stress by;

$$v = A e^{-(E + F\gamma)/k_B T} \quad (21)$$

where F is the applied force and γ is a constant. Shallamach only considered the influence of mechanical stress in the forward direction and thus predicted that the driving force will increase

logarithmically with the sliding velocity as described above. He noted the similarity of his approach to Eyring's in his paper.

Experiments subsequently showed that, after initially rising as $\log(\text{speed})$, rubber friction could then decrease with speed at high speeds and in 1963 Schallamach extended his model to account for this [23]. He treated polymer sliding as a process in which bonds between polymer molecules on the contacting surfaces are continually formed and ruptured. He retained equation 21 to describe the rate of bond rupture but introduced a different and much shorter relaxation time for bond reformation. At normal speeds, bonds effectively reform immediately but, at very high sliding speeds they do not have time to reform, so the shear stress for slip and thus the friction is reduced.

Schallamach's approach has been used quite extensively in recent years as the starting point for the development of friction models for a range of sliding contact types. The concept of sliding taking place due to motion of atoms or molecular groups over energy barriers has been broadened to consider sliding as resulting from the incoherent shearing and reformation of nano-domains or "junctions" as a surface moves against its counterface. Each junction is stretched until it either breaks due to thermal excitation or by external force.

In 2003, Drummond *et al.* applied Schallamach's approach to model boundary lubrication and compared the predictions with friction measurements of mica surfaces lubricated by aqueous surfactant solutions [24]. In addition to Schallamach's (and Eyring and Prandtl's) principle, that applied force reduces the energy barrier, thus allowing more rapid junction breaking, Drummond *et al.* also assumed that all junctions will break when they reached a critical elastic deformation. Mazuyer *et al.* have recently applied Drummond's model to the measured friction behaviour of solutions of two organic friction modifiers in polyalphaolefin base fluid in a surface forces apparatus [25].

3. NON-DEGENERATE INITIAL AND FINAL STATES: FRACTURE, TRIBOCHEMICAL REACTIONS AND WEAR

3.1 Fracture models

In 1941 Eyring and Tobolsky applied Eyring's absolute reaction rate model to describe the rupture and formation of bonds between polymer chains and thus to the creep of polymers [26]. In subsequent years this was extended by Coleman to describe polymer creep failure [27] and Zhurkov to model the fracture properties of a wide range of materials including metals, polymers and ceramics [28]. Zhurkov considered the fracture of a solid to be a time-dependent process whose rate is determined by mechanical stress and temperature and related the time to fracture to the applied stress, σ , in a form that will, by now be familiar to the reader;

$$\tau = \tau_0 e^{[(U_0 - \gamma\sigma)/k_B T]} \quad (22)$$

where τ_0 is the reciprocal of the natural oscillation frequency of atoms in the solid and U_0 is the magnitude of the energy barrier to break bonds in the solid. This barrier is assumed to decrease linearly with applied load under tensile stress σ . Zhurkov's Equ. 22, which neglects any bond reformation process was confirmed by experiments on several metals and polymers. With the advent of fracture mechanics, this approach was subsequently applied to model crack propagation rate [29,30].

3.2 Tribochemical Reactions and the Bell Model

Zhurkov's equation was also used by Bell in 1978 to model to adhesion of cells and the forces required to separate them [31]. His model, often called the "Bell model" has subsequently been quite widely adopted by researchers concerned with the influence of external forces on chemical bond breakage, i.e. the field of "mechanochemistry." In this case, the effect of an external force F increases the thermal reaction rate constant k_0 to yield a rate constant under the influence of a force $k(F)$ as;

$$k(F) = k_0 e^{F\Delta x^\ddagger/k_B T} \quad (23)$$

where Δx^\ddagger is the distance along the reaction coordinate from the initial to the transition state. Much of this research is concerned with the effect of tensional forces and is of no direct relevance to tribology although it includes study of the effect of applied stress on the rupture of linear polymers [32,33], which has considerable application to permanent shear stability of viscosity-modified lubricants.

3.2 Nanoscale Wear

Similar activation energy models have been used to describe dissolution [34] and nanoscale wear rates measured in an AFM [35-38]. In these models it is assumed that small clusters of atoms are removed from the surface by the AFM tip during sliding. The rate of atom loss due to wear $\Gamma_{atom-loss}$ (in units of s^{-1}) is assumed to be an activated process and modelled using transition-state theory;

$$\Gamma_{atom-loss} = \Gamma_0 \exp\left(-\frac{\Delta G_{act}}{k_B T}\right) \quad (24)$$

where Γ_0 is a pre-exponential factor (analogous to $1/\tau$ in Equ. 3 and R in Equ. 9). The effect of a stress component σ is assumed to lower the activation barrier and is written as $\Delta G_{act} = \Delta U_{act} - \sigma\Delta V_{act}$ where ΔV_{act} is the activation volume. This leads to an overall equation for the wear rate;

$$\Gamma_{atom-loss} = \left\{ \Gamma_0 \exp\left(-\frac{\Delta U_{act}}{k_B T}\right) \right\} \exp\left(\frac{\sigma\Delta V_{act}}{k_B T}\right) \quad (25)$$

where ΔU_{act} is an internal energy of activation. This predicts an exponential increase in nanoscale wear rate with contact stress, σ , and this has been found to be the case experimentally for a

number of systems. Fits to the data allow ΔU_{act} and ΔV_{act} to be estimated leading to physically reasonable values of ΔU_{act} from ~ 0.35 to 1.0 eV (~ 34 to 96 kJ/mol) and ΔV_{act} varying from 37 to 350 \AA^3 . However, since this wear process is likely to be relatively complex it is difficult to relate the value of ΔV_{act} , which corresponds to some volume change in going from the initial to the transition state, to some clearly identifiable physical process.

4. DISCUSSION

4.1 Comparison of Prandtl and Eyring models

From the above it can be seen that the original works of Prandtl [1] and Eyring [2] underpin all subsequent developments in the field. While the general concepts used by Prandtl and Eyring are similar in the sense that they both describe the lowering of the barrier of a thermally activated process by an external force, it is of interest to compare the two models and see how they differ and the extent to which they can be reconciled. It should be noted that in a recent “Retrospective” that accompanied their English translation of Prandtl’s paper [39], Popov and Gray ascribed Eyring’s Equ. 12 directly to Prandtl, although without explanation.

There appear to be three main differences between the models. The most significant is that Prandtl combines the sinusoidal potential of the counterface with the elastically-constrained “point mass” to obtain a new potential surface, in effect allowing the work done on the point mass to influence the shape of the energy barrier. His $(A-Bx)$ approximation (Equ. 5) assumes that the combined energy barrier decreases linearly with force \times distance as the force approaches the critical value at which the energy barrier becomes zero. This is superficially similar to Eyring who also assumes that the energy barrier reduces linearly with the product of applied force and distance moved. However Eyring’s linear variation represents the work carried out by the particle as it moves from the initial to the transition state; the energy barrier itself does not distort. This suggests that Eyring is most appropriate at relatively low applied forces compared to the maximum.

The second difference, quite closely related to the first, concerns the force experienced by a particle as it driven towards the energy barrier, and thus the work done on this particle. Prandtl assumes that the constraining force is elastic and so varies linearly with displacement. This is arguably appropriate for crystalline solids with short range attractive forces. By contrast, Eyring assumes the force is constant so that the work done is simply the product of force \times distance. This is perhaps appropriate to materials with weaker, longer range inter-particle forces, including organic liquids. These two quite different assumptions are analysed in detail later in this paper.

The third difference is that Prandtl assumes that sliding results from the simultaneous, forced transition across an energy barrier of many particles in a surface. He assumes that these elastically-constrained particles can, depending on their thermal energy, undergo transition from all positions as they are forced up the energy barrier. This assumption necessitates the use of a fraction term, μ in Equ. 3 along with the integration of this term to determine the relationship

between overall applied force and sliding speed. By contrast Eyring simply assumes that all particles move the same distance from the bottom of a potential well to the transition state, which corresponds to the mid-point of the energy barrier. Eyring's general approach is also that adopted by Shallamach (Equ. 22) and Bell (Equ. 24) and for fracture (Equ. 23) and nanoscale wear (Equ. 26) models. The simplicity of Eyring's approach means that it is possible to combine forward and reverse flow rates in equations that are analytically tractable.

In recent years, one of the main applications of Prandtl's model has been to describe the sliding of an AFM tip across a surface. Here the atoms or molecules in the surface are assumed to provide a periodically varying potential, equivalent to the undulating stationary surface in Fig. 1, while the tip represents the point mass. Whereas in Prandtl's analysis the spring force on the point mass originates from internal inter-particle forces, in the AFM analogy the cantilever acts as an external, restraining spring. Because there is just one sliding "point mass", Prandtl's concept of a fraction of particles available to undergo transition at a given position can be discarded, though the probability of transition as a function of position relative to the peak of the energy barrier is still relevant. The cantilever spring is generally assumed to be perfectly elastic with force constant k giving an external potential given by $V_e(x) = -\frac{1}{2}(x - X)^2$ where X describes the position of the end of the spring (corresponding to the cantilever position).

In an analogous approach for the constant-force sliding assumed by Eyring, $V_e(x) = -Fx$, where F is the constant force. In both cases, the full potential results from a combination of a surface corrugation, invariably assumed to be sinusoidal, plus V_e . The resulting decrease in barrier height as a function of force $\Delta E(F)$ cannot be derived analytically in either of these cases so that the next section in the following discussion focuses on deriving asymptotic solutions for both types of spring.

From section 2.1 it should be clear that a distinction must be made between the Prandtl-Tomlinson model, which considers the lowering in activation barrier resulting from the forces acting on a point mass moving over a periodic potential, and the Prandtl and Eyring "kinetic effects" which examine the influence of applied forces on thermal activation. The last section below considers the consequent temperature and velocity dependences for sliding from for the two models with constant-force (Eyring) and compliant (Prandtl) sliding.

The terminology used below is that now usually employed when applying Prandtl's approach to model AFM friction. To assist the reader, Table 1 compares this with the nomenclatures employed by Prandtl, Eyring and other previous researchers. It should be noted that Briscoe and Zhurkov, and also recent wear modelling, use an activation volume accompanied by an applied stress rather than a critical distance accompanied by an applied force.

	This Work	Prandtl [1]	Eyring [2]	Schallamach [22][23]	Briscoe [19]	Zhurkov [28]
Activation barrier height (J)	E_0	$A.k_B T$	E_0	E	Q'	U_0
Periodicity (m)	a	l	λ	-	b	-
Sliding velocity (m/s)	v	c	ΔV	v	v	-
Critical distance (m)	x^*, d	a	$\lambda/2$	γ	ϕ (vol.)	γ (vol.)
Critical force (N)	F^*	P_{max}	-	-	-	-
Transition time (s)	-	τ	-	τ_0	\square	τ_0
Attempt frequency (s^{-1})	f_0	-	k_1	-	v	-

Table 1: List of symbols used in the various models discussed above.

4.2 Dependence of Activation Energy on Force

4.2.1 Force Dependent Energy Barrier for a Compliant Contact; A Modern Description of the Prandtl/Tomlinson Model.

Because of the extensive use of AFM to measure nanoscale friction, the Prandtl-Tomlinson model has been fully discussed elsewhere [7-10,40,41] and will only be briefly summarized here. The surface energy profile is assumed to be sinusoidal, and is written as $-\frac{E_0}{2} \cos\left(\frac{2\pi x}{a}\right)$, where E_0 is the activation barrier height, a its periodicity and x is the position of the AFM tip on the surface. Combining this with an elastic potential cantilever with an effective force constant k_{eff} with a tip support that is moving at some constant scanning velocity v , $X = vt$, the combined time-dependent potential is given by;

$$V(x, t) = -\frac{E_0}{2} \cos\left(\frac{2\pi x}{a}\right) + \frac{1}{2} k_{eff} (x - vt)^2 \quad (26)$$

The shape of the potential depends on the height of the energy corrugation and the effective force constant; a large force constant yields a potential that is similar to a parabola, while a small force constant yields a more sinusoidal shape. This effect is captured by using a corrugation factor γ defined as;

$$\gamma = \frac{2\pi^2 E_0}{k_{eff} a^2} \quad (27).$$

In this model, the critical tip distance x^* (equivalent to a in Prandtl's paper) is the point at which the potential in equation (26) has an inflection to give;

$$\frac{x^*}{a} = \frac{1}{2\pi} \arccos\left(-\frac{1}{\gamma}\right) \quad (28).$$

In this picture, the force increases as the tip moves, giving rise to stick-slip behaviour, so that spontaneous sliding occurs at a critical distance x^* , which corresponds to a critical force given by;

$$F^* = \frac{k_{eff}a}{2\pi} \sqrt{\gamma^2 - 1} \quad (29)$$

As pointed out by Prandtl, an asymptotic solution as F approaches F^* can be written as;

$$\Delta E(F) = \frac{1}{\beta} (F^* - F)^{3/2} \quad (30)$$

where β is a constant given by [41];

$$\beta = \frac{(F^*)^{3/2}}{\left(\frac{k_{eff}a^2}{8} + \frac{F^*a}{\pi}\right)} \quad (31).$$

Equations 29 to 31 provide the necessary definitions of $\Delta E(F)$ and F^* required to predict the relationship between sliding velocity, temperature and friction force for an elastically-constrained AFM tip using Prandtl's thermal activation model, as described in section 4.2.1 below.

4.1.2 Force-Dependent Energy Barrier for Constant Force Sliding.

Eyring, Shallamach and Bell all assume that the shape of the surface potential is not influenced by the external force, and that the energy barrier is reduced by an amount equal to the external work $F \times d$ as the contact moves through a distance d under a constant applied force, F . If d is equal to the distance from the initial minimum in the potential to its maximum (the transition state) d^* (identical Prandtl's a), then the activation barrier reduces to zero at F^* so that $E_0 - F^* \times d^* = 0$ where E_0 is the barrier height. At some intermediate force F , $\Delta E(F) = E_0 - Fd^*$, which is the basic model adopted in the above theories.

Clearly this constant-force approach is not really appropriate for analysing AFM motion, where the cantilever is always elastic, but it is relevant to some forms of macroscopic sliding. However if we assume a constant force AFM cantilever we can derive asymptotic solutions for the variation in barrier height $\Delta E(F)$ as a function of a constant force F in a similar fashion to the elastic force case outlined above.

In the following, this model is explored using a combined sliding potential given by;

$$V(x, F) = \frac{E_0}{2} \left(1 - \cos\left(\frac{2\pi x}{a}\right)\right) - Fx \quad (32)$$

where E_0 is the height of the periodic potential with periodicity a , similar to that used in Equ. 26. Equ. (32) is similarly analyzed by calculating the height of the barrier as a function of the

external force, F . Increasing F reduces the height of the barrier, where the maxima and minima occur at turning points of Equ. 30 given by;

$$\left. \frac{\partial V}{\partial x} \right|_F = \frac{\pi E_0}{a} \sin\left(\frac{2\pi x}{a}\right) - F = 0 \quad (33).$$

The values of x at the maxima and minima are given by the solutions of $\sin\left(\frac{2\pi x}{a}\right) = \frac{Fa}{\pi E_0}$, which cannot be solved analytically; asymptotic solutions must be sought and will be derived for two force regimes. In the first, it is assumed that the barrier height is such that $E_0/k_B T$ is relatively small, so that small values of F cause a relatively large change in rate. This clearly applies well to the analysis of viscosity by Eyring since the molecules can thermally diffuse in the liquid. This force should also be much lower than the maximum force F^* at which spontaneous sliding occurs. This is given when the combined potential in Equ. 32 has a point of inflection; $\left. \frac{\partial^2 V}{\partial x^2} \right|_F = \frac{2\pi^2 E_0}{a^2} \cos\left(\frac{2\pi x}{a}\right) = 0$ to yield $x^* = \frac{a}{4}$, and $F^* = \frac{\pi E_0}{a}$.

We now calculate $\Delta E(F)$ for $F \ll F^*$. At $F=0$, Equ 32 reduces to a simple cosine function where the initial potential minimum is at $x_{min}=0$ with $E_{min}=0$, and a maximum at $x_{max}=\pi$ with $E_{max}=E_0$. As the force increases, x_{min} increases from zero and is given by the solution to Equ. 33. Expanding the sine function in Equ. 33 as a Taylor series for small values of F , and therefore small values of x_{min} , gives to first order: $\sin\left(\frac{2\pi x_{min}}{a}\right) \cong \frac{2\pi x_{min}}{a} = \frac{Fa}{\pi E_0}$ and yields $x_{min} = \frac{Fa^2}{2\pi^2 E_0}$. Substituting into equation (32) gives the energy of the minimum in the potential as a function of F as:

$$E_{min} = -\frac{E_0}{4} \left(\frac{F}{F^*}\right)^2 \quad (34).$$

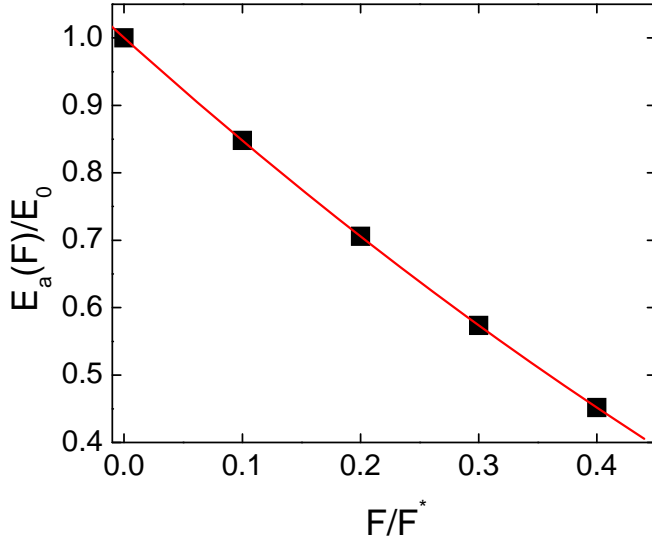


Figure 4: Plot of the relative height of the barrier under the influence of an external force F , scaled to F^* .

A similar analysis for the decrease in x_{max} from its initial value of π using a Taylor expansion of the sine function for small forces yields: $E_{max} = E_0 - \frac{Fa}{2} + \frac{E_0}{4} \left(\frac{F}{F^*}\right)^2$. The height of the energy barrier as a function of force $\Delta E(F)$ is the difference between the maximum and minimum energies;

$$\Delta E(F) = E_0 - \frac{Fa}{2} + \frac{E_0}{4} \left(\frac{F}{F^*}\right)^2 \quad (35).$$

Equ. 35 is shown plotted in Fig. 4, and is close to linear up values of $F/F^* \sim 0.4$, so that to a good approximation, $E_a(F) = E_0 - \frac{Fa}{2}$. This is identical to Eyring's assumption. It is interesting to note that the constant force model applies reasonably well even for relatively high forces, at least in the case of a simple sinusoidal potential, and provides some justification for its use by Schallamach. Equation 35 includes a quadratic term and a similar quadratic correction to the rigid-potential model has been proposed for mechanochemically induced reactions, to give what known as the extended-Bell model [42]. In this case, the quadratic force term is: $\frac{\chi^{TS} - \chi^{IS}}{2} F^2$, where χ is the compliance (the inverse of the force constant) at the transition and initial states, respectively. In the case of a sinusoidal surface potential, the values of χ^{TS} and χ^{IS} are identical, $\left(\frac{a^2}{2\pi^2 E_0}\right)$, but with opposite signs. Substituting into the above equation and scaling F to F^* gives $\frac{E_0}{2} \left(\frac{F}{F^*}\right)^2$ for the quadratic term, identical to Equ.35.

A general prediction of the Prandtl model is that the height of the energy barrier $\Delta E(F)$ should vary as $\Delta E \propto (F^* - F)^{3/2}$ as the external force F approaches F^* . This asymptote is explored for constant-force sliding (with a combined potential given by Equ. 30). Spontaneous sliding occurs at a lateral force $F^* = \frac{\pi E_0}{a}$ at a distance $x^* = \frac{a}{4}$. The value of the potential energy at the inflection point can be calculated by substituting these values into Equ. (30) to give: $V(x^*, F^*) = \frac{E_0}{2} - \frac{\pi E_0}{4}$. This is now expanded about x^* and F^* ; F is allowed to change from F^* to $F^* - \delta F$ so that $\delta F = F^* - F$. The variable x is rewritten as $x^* + \delta x$ so that $V(x, F) = V(x^*, F^*) + \delta V(\delta x)$. Substituting into equation (30) and substituting for F^* , x^* and $V(x^*, F^*)$ and writing $\cos\left(\frac{\pi}{2} + \frac{2\pi}{a}\delta x\right) = -\sin\left(\frac{2\pi}{a}\delta x\right)$ gives;

$$\delta V(\delta x) = \frac{E_0}{2} \sin\left(\frac{2\pi}{a}\delta x\right) - \frac{\pi E_0}{a}\delta x + \frac{a}{4}\delta F + \delta F\delta x \quad (36),$$

Expanding the sinusoidal potential as a Taylor series simplifies the equation to;

$$\delta V(\delta x) = -\frac{(2\pi)^3 E_0}{12a^3}(\delta x)^3 + \frac{a}{4}\delta F + \delta F\delta x \quad (37).$$

This is a third-order polynomial in δx about the inflection point, as expected. The difference between the maximum and minimum energies of Equ. 37 gives the height of the barrier $\Delta E(F)$ as the force approaches F^* . The maximum and minimum energies E_{max} and E_{min} are found by differentiating Equ.37, and the difference between these values equals $\Delta E(F)$;

$$\Delta E(F) = \frac{1}{\beta} (F^* - F)^{3/2} \quad (38),$$

where

$$\beta = \frac{3}{2\sqrt{2}} \frac{\sqrt{F^*}\pi}{a}. \quad (39).$$

Thus the asymptotic force dependence predicted by Prandtl is a general feature of force-activated sliding for both compliant and constant force external potentials, merely differing in the values of F^* and β .

4.2 Velocity and Temperature Dependence of Sliding Force

This section discusses how the asymptotic solutions for $\Delta E(F)$ are used to describe the velocity and temperature dependences of the friction force for both compliant and constant-force sliding by applying the thermal activation principle developed by Prandtl and Eyring. In both cases, the external force leads to a reduction in the remaining energy barrier, thereby increasing the transition rate. The characteristic time τ during which this can occur depends on the sliding speed v and periodicity a of the surface potential (in Eqs. 26 and 32) where $\tau \sim \frac{a}{v}$. The force F then adjusts so that the transition over the barrier occurs during the time τ . Since $\Delta E(F)$

decreases with increasing F , the force must increase as τ becomes smaller so that higher velocities result in larger friction forces.

All sliding friction models assume an Arrhenius temperature dependence of the rate; higher temperatures result in higher transition rates. Thus, as the temperature increases, the transition can occur for larger values of $\Delta E(F)$, resulting in a reduction in friction force with increasing temperature. These general concepts apply to both a compliant contact (e.g. in an AFM) and constant-force sliding where the constraining force is usually applied internally. For a compliant contact, the force increases as sliding occurs to produce a force that increases with time until the system transits the barrier, resulting in stick-slip motion that is characteristic of AFM friction experiments.

4.2.1 Velocity and Temperature Dependence for a Compliant Contact

The solution of the thermally-activated, modified Prandtl model for AFM friction has been discussed in detail elsewhere [43,44,9,45,41,46,21,39] and is briefly summarized here. The probability $p(t)$ that the tip surmounts the barrier is calculated following Prandtl for a forward jump from;

$$\frac{dp(t)}{dt} = -f_0 \exp\left(-\frac{\Delta E(t)}{k_B T}\right) p(t) \quad (40)$$

where the attempt time τ used by Prandtl (Equ. 3) is replaced by an attempt frequency f_0 . (Note that unlike Prandtl's μ , probability $p(t)$ is not the fraction of particles that undergo transition at time t , but the probability that the tip has not jumped by time t in its approach to the energy barrier). Since the lateral force F is measured in the AFM experiment, it is most convenient to cast this equation as a function of F rather than t to give;

$$\frac{dp(F)}{dF} = -f_0 \exp\left(-\frac{\Delta E(F)}{k_B T}\right) \left(\frac{dF}{dt}\right)^{-1} p(F) \quad (41).$$

Writing $\frac{dF}{dt} = \frac{dF}{dx} \frac{dx}{dt} \approx k_{eff} v$ gives a simple first-order differential equation;

$$\frac{dp(F)}{dF} = -\frac{f_0}{k_{eff} v} \exp\left(-\frac{\Delta E(F)}{k_B T}\right) p(F) \quad (42).$$

The variation in barrier height with force, $\Delta E(F)$ is usually taken to be the asymptotic form suggested by Prandtl, $\Delta E(F) \propto (F^* - F)^{3/2}$ (see Section 4.2.1.). Rather than integrating the equation as attempted by Prandtl (in approximate form), it is recognised that the peak force for the stick-slip motion seen in AFM experiments occurs when the transition rate is maximum and is calculated from $\frac{d^2 p}{dF^2} = 0$. For $\gamma > 4.603$, this yields a solution for the temperature and velocity dependence of the friction force as;

$$\frac{1}{\beta k_B T} (F^* - F)^{3/2} = \ln\left(\frac{v}{v_0}\right) - \frac{1}{2} \ln\left(1 - \frac{F}{F^*}\right) \quad (43)$$

where $v_0 = \frac{2f_0\beta k_B T}{3k_{eff}\sqrt{F^*}}$. This equation predicts essentially identical temperature and velocity dependences as found by Prandtl. As expected, it results in a logarithmic velocity dependence and a decrease in friction force with increasing temperature, and the velocity and temperature dependences predicted by Equ. 43 have been confirmed experimentally [47,10].

4.2.2 Velocity- and Temperature-Dependent Friction for a Constant Force Contact

As noted above, at a sliding velocity v the force F adjusts to lower the activation barrier such that the increased transition rate R allows the system to overcome the barrier. If the periodicity along the sliding direction is a , then;

$$v = Ra \quad (44).$$

If the barrier height under the influence of the external force is $\Delta E(F)$, which decreases as F increases, at some temperature T , the rate is given by;

$$R = A \exp\left(-\frac{\Delta E(F)}{k_B T}\right) \mu \quad (45),$$

where we use Prandtl's notation for the occupancy μ of the initial state and A is a preexponential factor (equivalent to f_0 in Equ. 41). For the shear of a contacting liquid interface, all the minima are occupied, so that $\mu \sim 1$ as used by Eyring. In the case of a nano-scale contact, where an atom slides from one minimum to the next, μ then depends on time and the full rate equation must be solved. With the assumption of $\mu \sim 1$, substituting Equ. (45) into Equ. (44) gives: $v = aA \exp\left(-\frac{\Delta E(F)}{k_B T}\right)$.

Note that, if the activation energy without the external force E_a is small (a few times $k_B T$) as in the Eyring model, the system can diffuse in both directions to the next site in the absence of an external force, but here the net motion is zero. To take account of the reverse jumps, Equ. (44) is modified to: $v = (R_f - R_b)a$ where R_f and R_b are the forward and back rates, and is used in the Eyring model (Section 2.2). Assuming for simplicity that sliding only accelerates the forward rate gives;

$$\Delta E(F) = k_B T \ln\left(\frac{v_c}{v}\right) \quad (46),$$

where $v_c = Aa$, and significant velocity dependences will only be seen for $v < v_c$. Explicit solutions depend on the form of $\Delta E(F)$. If we take the low-force limit where $\Delta E(F) = E_0 - \frac{Fa}{2}$, then;

$$F(v, T) = \frac{2E_0}{a} - \frac{2k_B T}{a} \ln\left(\frac{v_c}{v}\right) \quad (47).$$

However, if the barrier is larger, then higher forces are required to decrease the barrier such that $\Delta E(F) = \frac{1}{\beta} (F^* - F)^{3/2}$, so that;

$$F(v, T) = F^* - (\beta k_B T)^{2/3} \left(\ln \left(\frac{v_c}{v} \right) \right)^{2/3} \quad (48).$$

Again, both models predict a logarithmic dependence of friction force on velocity and an approximately linear decrease with increasing temperature.

4. CONCLUSIONS

It is clear that a remarkable range of tribological phenomena can be described by models in which the rate of a thermally activated process is accelerated by the application of an external force so that mechanical energy directly couples into the process to effectively lower the activation barrier. Such models in various forms have been used to describe viscosity, solid sliding, tribochemical reaction rates and even nano-scale wear. All of these models appear to derive inspiration from two original sources, a paper on crystal plasticity in 1928 by Prandtl and one on liquid viscosity in 1936 by Eyring.

There is, however, some confusion in the literature as to the origins of the thermal activation concept. This is probably because Prandtl essentially developed two separate models in his 1928 paper [1]. One explains irreversible flow and sliding in terms of instabilities in the forces experienced by elastically constrained particles in a surface as they move past a periodically varying potential. In the following year a very similar concept was developed by Tomlinson [2] and their combined efforts are now generally called the Prandtl-Tomlinson model. Prandtl's second development was to couple the effects of applied force and temperature on particle motion with the concept of "thermal activation". This enables prediction of the dependence of flow and sliding on applied force and the effects on both of changes in temperature. Unfortunately this development is also sometimes, incorrectly, included under the umbrella of "Prandtl-Tomlinson". In 1936 Eyring, arriving from a very different scientific direction, independently developed the thermal activation approach to produce a model of liquid viscosity, and until recently it has been Eyring's work rather than Prandtl's that has been most widely applied in subsequent tribology research. Perhaps the general principle of thermally-activated, stress induced processes in tribology might be best described as Prandtl-Eyring.

In many cases, thermally activated models are difficult to test experimentally since all the rate equations depend on the temperature of the system. The latter is, in general, extremely difficult to measure at a tribological interface so that the models tend to work best under relatively mild conditions where any increase in surface temperature due to frictional heating is negligible. Measuring the temperature dependences of the rates predicted for various processes by these models by making Arrhenius plots, as is commonly done for chemical reaction kinetics, is similarly hampered by difficulties measuring interfacial temperatures.

Another, more subtle issue is that the rate laws used to describe the phenomena invariably assume that the system is in thermal equilibrium so that the energy distribution is described by a Boltzmann function (i.e., $\sim \exp(-E/k_B T)$). Molecular dynamics simulations have suggested that significant deviations from thermal equilibrium can occur at sliding interfaces [48]. The models all inherently assume that all of the energy is rapidly dissipated after transiting the energy barrier, which may not always be the case.

Nevertheless, models that describe the direct coupling of mechanical energy into an activated process have been remarkably successful at describing a wide range of tribological phenomena and, we believe, will provide a powerful strategy for obtaining a molecular-level understanding of energy dissipation, tribochemistry and wear in the future.

ACKNOWLEDGEMENTS We thank the National Science Foundation for partial support of this work under grant number CMMI-1265742

5. REFERENCES

1. Prandtl, L.: Ein Gedankenmodell zur kinetischen Theorie der festen Körper. *Z. Angew. Math. Mech.* **8**, 85 (1928).
2. Eyring, H.: Viscosity, Plasticity, and Diffusion as Examples of Absolute Reaction Rates. *The Journal of Chemical Physics* **4**(4), 283-291 (1936).
3. Hill, T.L.: *Statistical mechanics : principles and selected applications*. McGraw-Hill, New York (1956)
4. Prigogine, I.: *Introduction to thermodynamics of irreversible processes*. Interscience Publishers, New York (1968)
5. Huang, K., Szlufarska, I.: Green-Kubo relation for friction at liquid-solid interfaces. *Physical Review E* **89**(3), 032119 (2014).
6. Tomlinson, G.A.: A Molecular Theory of Friction. *Phil. Mag.* **7**, 905 (1929).
7. Gnecco, E., Bennewitz, R., Gyalog, T., Meyer, E.: Friction experiments on the nanometre scale. *Journal of Physics-Condensed Matter* **13**(31), R619-R642 (2001).
8. Bennewitz, R., Gnecco, E., Gyalog, T., Meyer, E.: Atomic friction studies on well-defined surfaces. *Tribology Letters* **10**(1), 51-56 (2001).
9. Gnecco, E., Bennewitz, R., Socoliuc, A., Meyer, E.: Friction and wear on the atomic scale. *Wear* **254**(9), 859-862 (2003).
10. Riedo, E., Gnecco, E., Bennewitz, R., Meyer, E., Brune, H.: Interaction Potential and Hopping Dynamics Governing Sliding Friction. *Physical Review Letters* **91**(8), 084502 (2003).
11. Filleter, T., Paul, W., Bennewitz, R.: Atomic structure and friction of ultrathin films of KBr on Cu(100). *Physical Review B* **77**(3), 035430 (2008).
12. Müser, M.H.: Lubricants under high local pressure: Liquids act like solids. *Materialwissenschaft und Werkstofftechnik* **35**(10-11), 603-609 (2004).
13. Eyring, H.: The Activated Complex in Chemical Reactions. *The Journal of Chemical Physics* **3**(2), 107-115 (1935).
14. Ewell, R.H.: The Reaction Rate Theory of Viscosity and Some of its Applications. *Journal of Applied Physics* **9**(4), 252-269 (1938).

15. Kauzmann, W., Eyring, H.: The Viscous Flow of Large Molecules. *Journal of the American Chemical Society* **62**(11), 3113-3125 (1940).
16. Karis, T.E., Nagaraj, H.S.: Evaporation and Flow Properties of Several Hydrocarbon Oils. *Tribol. Trans.* **43**(4), 758-766 (2000).
17. Ree, F., Ree, T., Eyring, H.: Relaxation Theory of Transport Problems in Condensed Systems. *Industrial & Engineering Chemistry* **50**(7), 1036-1040 (1958).
18. Tevaarwerk, J., Johnson, K.L.: A simple non-linear constitutive equation for elastohydrodynamic oil films. *Wear* **35**(2), 345-356 (1975).
19. Briscoe, B.J., Evans, D.C.B.: The Shear Properties of Langmuir-Blodgett Layers. *Proceedings of the Royal Society of London. A. Mathematical and Physical Sciences* **380**(1779), 389-407 (1982).
20. Bouhacina, T., Aimé, J., Gauthier, S., Michel, D., Heroguez, V.: Tribological behavior of a polymer grafted on silanized silica probed with a nanotip. *Physical Review B* **56**(12), 7694-7703 (1997).
21. Müser, M.: Velocity dependence of kinetic friction in the Prandtl-Tomlinson model. *Physical Review B* **84**(12), 125419 (2011).
22. Schallamach, A.: The Velocity and Temperature Dependence of Rubber Friction. *Proceedings of the Physical Society. Section B* **66**(5), 386 (1953).
23. Schallamach, A.: A theory of dynamic rubber friction. *Wear* **6**(5), 375-382 (1963).
24. Drummond, C., Israelachvili, J., Richetti, P.: Friction between two weakly adhering boundary lubricated surfaces in water. *Physical Review E* **67**(6), 066110 (2003).
25. Mazuyer, D., Cayer-Barrioz, J., Tonck, A., Jarnias, F.: Friction Dynamics of Confined Weakly Adhering Boundary Layers. *Langmuir* **24**(8), 3857-3866 (2008).
26. Tobolsky, A., Eyring, H.: Mechanical Properties of Polymeric Materials. *The Journal of Chemical Physics* **11**(3), 125-134 (1943).
27. Coleman, B.D.: Application of the theory of absolute reaction rates to the creep failure of polymeric filaments. *Journal of Polymer Science* **20**(96), 447-455 (1956).
28. Zhurkov, S.N.: Kinetic concept of the strength of solids. *International Journal of Fracture Mechanics* **1**, 11 (1965).
29. Henderson, C.B., Graham, P.H., Robinson, C.N.: A comparison of reaction rate models for the fracture of solids. *International Journal of Fracture Mechanics* **6**(1), 33-40 (1970).
30. Pollet, J.C., Burns, S.J.: Thermally activated crack propagation — theory. *Int J Fract* **13**(5), 667-679 (1977).
31. Bell, G.: Models for the specific adhesion of cells to cells. *Science* **200**(4342), 618-627 (1978).
32. Sohma, J.: Mechanochemistry of polymers. *Progress in Polymer Science* **14**(4), 451-596 (1989).
33. Wiggins, K.M., Brantley, J.N., Bielawski, C.W.: Polymer Mechanochemistry: Force Enabled Transformations. *ACS Macro Letters* **1**(5), 623-626 (2012).
34. Dickinson, J.T., Park, N.S., Kim, M.W., Langford, S.C.: A scanning force microscope study of a tribochemical system: stress-enhanced dissolution. *Tribology Letters* **3**(1), 69-80 (1997).
35. Jacobs, T.D.B., Carpick, R.W.: Nanoscale wear as a stress-assisted chemical reaction. *Nat Nano* **8**(2), 108-112 (2013).
36. Gotsmann, B., Lantz, M.A.: Atomistic Wear in a Single Asperity Sliding Contact. *Physical Review Letters* **101**(12), 125501 (2008).

37. Jacobs, T.B., Gotsmann, B., Lantz, M., Carpick, R.: On the Application of Transition State Theory to Atomic-Scale Wear. *Tribology Letters* **39**(3), 257-271 (2010).
38. Kopta, S., Salmeron, M.: The atomic scale origin of wear on mica and its contribution to friction. *The Journal of Chemical Physics* **113**(18), 8249-8252 (2000).
39. Popov, V.L., Gray, J.A.T.: Prandtl-Tomlinson model: History and applications in friction, plasticity, and nanotechnologies. *ZAMM - Journal of Applied Mathematics and Mechanics / Zeitschrift für Angewandte Mathematik und Mechanik* **92**(9), 683-708 (2012).
40. Socoliuc, A., Bennewitz, R., Gnecco, E., Meyer, E.: Transition from Stick-Slip to Continuous Sliding in Atomic Friction: Entering a New Regime of Ultralow Friction. *Physical Review Letters* **92**(13), 134301 (2004).
41. Furlong, O.J., Manzi, S.J., Pereyra, V.D., Bustos, V., Tysoe, W.T.: Kinetic Monte Carlo theory of sliding friction. *Physical Review B* **80**(15) (2009).
42. Konda, S.S.M., Brantley, J.N., Bielawski, C.W., Makarov, D.E.: Chemical reactions modulated by mechanical stress: Extended Bell theory. *The Journal of Chemical Physics* **135**(16), 164103-164108 (2011).
43. Sasaki, N., Tsukada, M., Fujisawa, S., Sugawara, Y., Morita, S.: Theoretical analysis of atomic-scale friction in frictional-force microscopy. *Tribology Letters* **4**(2), 125-128 (1998).
44. Porto, M., Zaloj, V., Urbakh, M., Klafter, J.: Macroscopic versus microscopic description of friction: from Tomlinson model to shearons. *Tribology Letters* **9**(1), 45-54 (2000).
45. Fusco, C., Fasolino, A.: Velocity dependence of atomic-scale friction: A comparative study of the one- and two-dimensional Tomlinson model. *Physical Review B* **71**(4), 045413 (2005).
46. Furlong, O.J., Manzi, S.J., Pereyra, V.D., Bustos, V., Tysoe, W.T.: Monte Carlo Simulations for Tomlinson Sliding Models for Non-Sinusoidal Periodic Potentials. *Tribology Letters* **39**(2), 177-180 (2010).
47. Gnecco, E., Bennewitz, R., Gyalog, T., Loppacher, C., Bammerlin, M., Meyer, E., Güntherodt, H.J.: Velocity Dependence of Atomic Friction. *Physical Review Letters* **84**(6), 1172-1175 (2000).
48. Mazyar, O.A., Xie, H., Hase, W.L.: Nonequilibrium energy dissipation at the interface of sliding model hydroxylated alpha-alumina surfaces. *The Journal of Chemical Physics* **122**(9), 094713-094712 (2005).